



MISSOURI
S&T

CENTER FOR TRANSPORTATION INFRASTRUCTURE AND SAFETY



Miniaturized Fiber Inline Fabry-Pérot Interferometer for Chemical Sensing

by

Tao Wei and Hai Xiao



**NUTC
R203**

**A National University Transportation Center
at Missouri University of Science and Technology**

Disclaimer

The contents of this report reflect the views of the author(s), who are responsible for the facts and the accuracy of information presented herein. This document is disseminated under the sponsorship of the Department of Transportation, University Transportation Centers Program and the Center for Transportation Infrastructure and Safety NUTC program at the Missouri University of Science and Technology, in the interest of information exchange. The U.S. Government and Center for Transportation Infrastructure and Safety assumes no liability for the contents or use thereof.

Technical Report Documentation Page

1. Report No. NUTC R203	2. Government Accession No.	3. Recipient's Catalog No.	
4. Title and Subtitle Miniaturized Fiber Inline Fabry-Pérot Interferometer for Chemical Sensing	5. Report Date January 2010		
	6. Performing Organization Code		
7. Author/s Tao Wei and Hai Xiao	8. Performing Organization Report No. 00016751		
9. Performing Organization Name and Address Center for Transportation Infrastructure and Safety/NUTC program Missouri University of Science and Technology 220 Engineering Research Lab Rolla, MO 65409	10. Work Unit No. (TRAIS)		
	11. Contract or Grant No. DTRT06-G-0014		
12. Sponsoring Organization Name and Address U.S. Department of Transportation Research and Innovative Technology Administration 1200 New Jersey Avenue, SE Washington, DC 20590	13. Type of Report and Period Covered Final		
	14. Sponsoring Agency Code		
15. Supplementary Notes			
16. Abstract This paper demonstrates the chemical sensing capability of a miniaturized fiber inline Fabry-Pérot sensor fabricated by femtosecond laser. Its accessible cavity enables the device to measure the refractive index within the cavity. The refractive index change introduced by changing the acetone solution concentration was experimentally detected with an error less than 4.2×10^{-5} .			
17. Key Words Fabry-Pérot interferometer, femtosecond laser, fiber-optic sensor, refractive index measurement	18. Distribution Statement No restrictions. This document is available to the public through the National Technical Information Service, Springfield, Virginia 22161.		
19. Security Classification (of this report) unclassified	20. Security Classification (of this page) unclassified	21. No. Of Pages 5	22. Price

Miniaturized Fiber Inline Fabry-Pérot Interferometer for Chemical Sensing

Tao Wei and Hai Xiao

Dept. of Electrical and Computer Eng., Missouri University of Sci. and Tech., MO, USA 65409

ABSTRACT

This paper demonstrates the chemical sensing capability of a miniaturized fiber inline Fabry-Pérot sensor fabricated by femtosecond laser. Its accessible cavity enables the device to measure the refractive index within the cavity. The refractive index change introduced by changing the acetone solution concentration was experimentally detected with an error less than 4.2×10^{-5} .

Keywords: Fabry-Pérot interferometer, femtosecond laser, fiber-optic sensor, refractive index measurement.

1. INTRODUCTION

Accurate refractive index measurement based optical sensing devices have raised a growing interest in recent years due to their broad applications in chemical and biological sensing. Preferably, these devices shall have a small size, high sensitivity, fast response time and large dynamic range. Many existing devices operate based on evanescent field interactions. Examples include long period fiber gratings, [1] chemically etch-eroded fiber Bragg gratings, [2] optical microresonators/microcavities, [3] fiber surface plasmon resonance (SPR) devices, [4] photonic crystals, [5, 6] etc. In general, these devices have shown high sensitivity for refractive index measurement. Characterized as the resonance wavelength shift in response to refractive index changes, it has been reported that LPFGs can provide a sensitivity as high as 6000nm/RIU (refractive index unit) while microresonators can reach 800nm/RIU. [7] However, the evanescent field-based devices have a nonlinear response to refractive index, meaning that the sensitivity varies at different refractive index ranges. The dynamic range of refractive index measurement is also limited. In addition, many existing devices have shown large temperature cross sensitivity. As a result, temperature induced errors need to be corrected in real time.

Low finesse fiber Fabry-Perot interferometers (FPI) have been widely used as optical sensors. In a fiber FPI, the phase of the interference signal is linearly proportional to the optical length of the cavity, defined as the product of the cavity length and the refractive index of the medium filling the cavity. When exposed to the external environment, a FPI cavity can be used to measure the refractive index by tracking the phase shift of the interference signal [8] However, so far fiber FPIs have not been widely used for refractive index sensing, mainly because they have been commonly made with a sealed cavity. [9-11] As a result, their applications have been limited to the measurement of physical parameters such as pressure, strain and temperature, etc. Very recently, we successfully fabricated a miniaturized fiber inline FPI by one-step machining of a micro-notch on a single mode optical fiber using a femtosecond (fs) laser. [12] The all-glass, inline FPI has small temperature dependence and more attractively, an open cavity that is accessible to the external environment. In this letter, we report our experimental investigations on its capability for temperature-insensitive refractive index sensing.

2. SENSOR FABRICATION

The device fabrication was carried out using a home-integrated fs laser 3D micromachining system as schematically shown in Fig. 1. The repetition rate, center wavelength and pulse width of the fs laser (Legend-F, Coherent, Inc.) were 1kHz, 800nm and 120fs, respectively. The maximum output power of the fs laser was approximately 1W. We used the combination of waveplates and polarizers to reduce the laser power to about 20mW, and then used several neutral density (ND) filters to further reduce the laser power to desirable values. The attenuated laser beam was directed into an objective lens (Olympus UMPLFL 20X) with a numerical aperture (NA) of 0.45 and focused onto the single mode optical fiber (Corning SMF 28) mounted on a computer-controlled five-axis translation stage (Aerotech, Inc.) with a resolution of 1 μ m.

During fabrication, the interference signal of the fiber FP device was continuously monitored. A tunable laser source (HP 8168E) was connected to one of the input ports of the 3dB fiber coupler. The output port of the coupler was connected to the device under fabrication. Controlled by the computer, the tunable laser continuously scanned through its wavelength range (1475-1575nm) at the rate of 1nm per step. The signal reflected from the device at each wavelength step was recorded by an optical power meter (Agilent 8163A). The fabrication was stopped after a well-formed interference pattern was recorded.

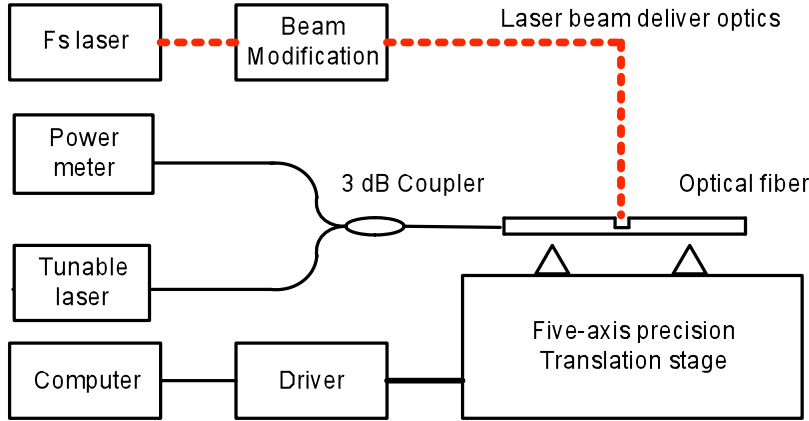


Fig. 1. Fiber inline FPI device fabrication system using a fs laser

Fig. 2 shows the structural schematic and the scanning electron microscope (SEM) image of the fabricated fiber inline FPI device. The cavity length was about 60 μm as estimated from the SEM image. The depth of micro-notch was around 72 μm , just passing the fiber core. The FP cavity was made very close ($\sim 2\text{mm}$) to the end of the fiber. With such a short bending arm, the chance of bending induced device breakage is small. The interference spectrum of the device in air is shown in Fig. 3. The background loss of this particular device was about 20dB. The interference spectrum indicated a fringe visibility of about 5dB, which is sufficient for most sensing applications.

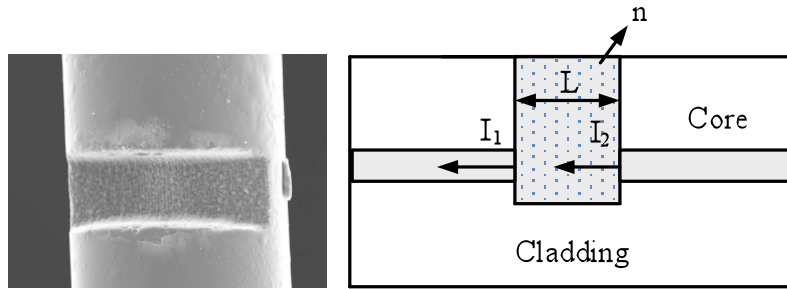


Fig. 2. Structural schematic and SEM image of the fiber FPI fabricated by fs laser micromachining.

Due to the low reflectivity of the laser-ablated surface, multiple reflections have negligible contributions to the optical interference. The low finesse FP device can thus be modeled using the two-beam optical interference equation [13]:

$$I = I_1 + I_2 + 2\sqrt{I_1 I_2} \cos\left(\frac{4\pi n \cdot L}{\lambda} + \phi_0\right) \quad (1)$$

where, I is the intensity of the interference signal; I_1 and I_2 are the reflections at the cavity surfaces, respectively; ϕ_0 is the initial phase of the interference; L is the length of the cavity; n is the refractive index of the medium filling the cavity; λ is the optical wavelength in vacuum.

According to Eq. (1), the two adjacent interference minimums have a phase difference of 2π . Therefore the optical length of the cavity can be calculated by:

$$L \cdot n = \frac{1}{2} \left(\frac{\lambda_1 \lambda_2}{\lambda_2 - \lambda_1} \right) \quad (2)$$

where λ_1 and λ_2 are the center wavelengths of two adjacent valleys (Fig. 3) in the interference spectrum. The length of the FP cavity was found to be $63.112\mu\text{m}$ when we set n to be 1.0008 for air. The calculated value was close to the length estimated by the SEM image.

3. EXPERIMENT AND DISCUSSION

To evaluate its capability for refractive index measurement, the fiber FPI device was immersed into various liquids including methanol, acetone and isopropanol at room temperature. The interrogation of the FPI sensor is shown in Fig. 4. A broadband source made by multiplexing a C-band and a L-band Erbium doped fiber ASE (amplified spontaneous emission) source was used to excite the device through a 3dB fiber coupler. The reflected interference signal from the sensor was detected by an optical spectrum analyzer (OSA, HP70952B). The spectral resolution of OSA was set to 0.5nm and 1600 data points were obtained per OSA scan.

The interference spectra are also shown in Fig. 3 for comparison. The interference intensity dropped when the device was immersed in liquids as a result of the reduced reflection from the cavity endfaces. However, the interference fringes maintained similar visibility. The spectral distance between the two adjacent valleys also decreased, indicating the increase of refractive index of the medium inside the cavity. Based on Eq. (1), the refractive indices of the liquids were calculated to be: $n_{\text{methanol}} = 1.3283$, $n_{\text{acetone}} = 1.3577$, and $n_{\text{isopropanol}} = 1.3739$, which were very close to the commonly accepted values.

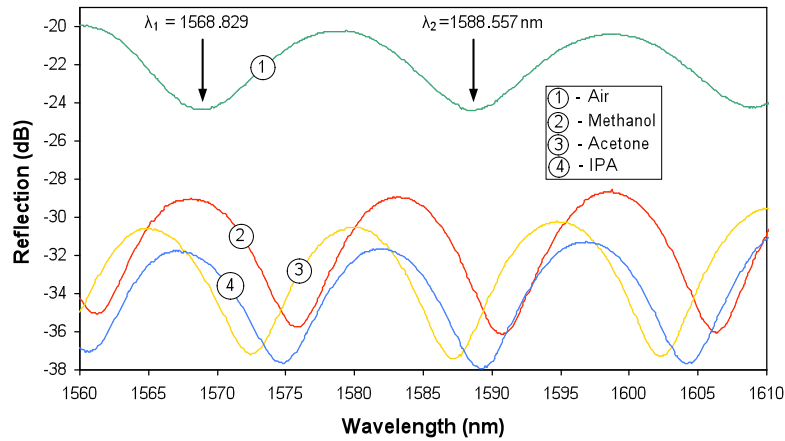


Fig. 3. Interference spectra of the FPI device in air, methanol, acetone and isopropanol.

We also studied the device's capability for temperature-insensitive refractive index sensing by measuring the temperature-dependent refractive index of deionized water. As shown in Fig. 4, the fiber device was attached to the tip of a thermometer and immersed into deionized water in a beaker. The beaker is placed in a large container for water/ice bath and the container was placed on a stirring/hot plate (Corning PC-420D). A magnetic stirrer was also used to equilibrate the temperature during experiment. The system was first heated till the water inside the beaker reached 90°C read from the thermometer. Then the heater was turned off to allow the system to cool down smoothly while the interference spectrum was recorded at every degree of temperature dropping. Ice was added into the water bath container to help cooling the system at low temperatures. The measurement ended till the temperature inside the beaker reached 3°C .

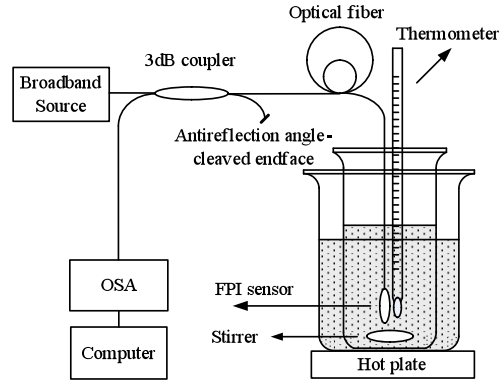


Fig. 4. Experimental setup for refractive index measurement.

Fig. 4 shows the measured refractive index of water as a function of temperature. As the temperature increases, the interference fringe shifts to a shorter wavelength indicating the decrease of the refractive index of water. Assuming a constant cavity length over the entire temperature range, we calculated the refractive index change based on the linear proportional relation between the amount refractive index change (Δn) and the wavelength shift ($\Delta\lambda_v$) of a particular interference valley, given by

$$\Delta n = \frac{\Delta\lambda_v}{\lambda_v} n \quad (3)$$

where λ_v is the wavelength of the specific interference valley.

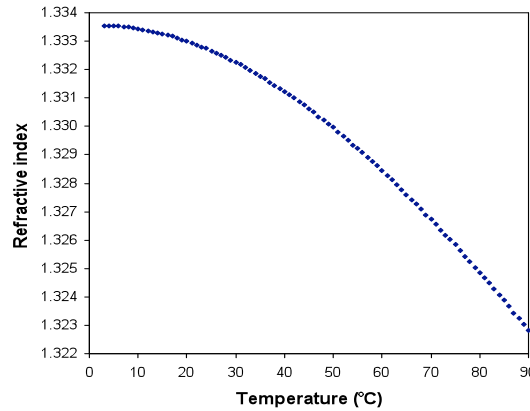


Fig. 5. Measured refractive index of deionized water as a function of temperature.

The measured refractive index of water as a function of temperature, shown in Fig. 5, agreed well with the previously reported measurements. [14] According to equation (3), the sensitivity for measurement of refractive index of water is estimated to be 1163nm/RIU at the wavelength of 1550nm. Given a spectral resolution of 10pm of the OSA, the detection limit was about 8.6×10^{-6} RIU.

We also conducted an experiment to evaluate the temperature cross sensitivity of the sensor. A temperature variation from 20 to 100°C in air caused a wavelength shift less than 0.1nm of the interference fringe. Without temperature

compensation, the maximum temperature-induced error was estimated to be 9.4×10^{-5} RIU for water refractive index measurement within the temperature range of 3 to 90°C [15].

4. CONCLUSION

In conclusion, we demonstrated a fiber inline FPI device with open cavity fabricated by one-step fs laser micromachining for highly sensitive refractive index measurement. The device was evaluated for refractive index measurement of various liquids and the results matched well with the reported data. The inline fiber FPI was also tested to measure the temperature-dependent refractive index of deionized water from 3 to 90°C with a sensitivity of 1163nm/RIU. The maximum temperature-induced error was 9.4×10^{-5} RIU within the entire temperature variation range. The small size, all-fiber inline structure, small temperature dependence, linear response, high sensitivity, and most attractively, an open cavity that is accessible to the external environment, make the new fiber inline FPI an attractive refractive index sensor that has many applications in chemical and biological sensing.

5. ACKNOWLEDGEMENT

The research work was supported by the Office of Naval Research through the Young Investigator Program (N00014-07-0008) and the University of Missouri Research Board (UMRB). Tao Wei is supported by the Missouri S&T National University Transportation Center Graduate Fellowship Program.

REFERENCES

- [1] Ignacio Del Villar, Ignacio R. Matias, and Francisco J. Arregui, "Enhancement of sensitivity in long-period fiber gratings with deposition of low-refractive-index materials," *Opt. Lett.* 30, 2363-2365 (2005).
- [2] W. Liang, Y. Huang, Y. Xu, R. K. Lee, and A. Yariv, "Highly sensitive fiber Bragg grating refractive index sensors," *Appl. Phys. Lett.* 86, Art. 151122 (2005).
- [3] I. M. White, H. Oveys, and X. Fan, "Liquid-core optical ring-resonator sensors," *Opt. Lett.* 31, 1319-1321 (2006).
- [4] Bertrand Gauvreau, Alireza Hassani, Majid Fassi Fehri, Andrei Kabashin, and Maksim A. Skorobogatiy, "Photonic bandgap fiber-based Surface Plasmon Resonance sensors," *Opt. Express* 15, 11413-11426 (2007).
- [5] N. Skivesen, A. Têtu, M. Kristensen, J. Kjems, L. H. Frandsen, and P. I. Borel, "Photonic-crystal waveguide biosensor," *Opt. Express* 15, 3169-3176 (2007).
- [6] Y. Nishijima, K. Ueno, S. Juodkazis, V. Mizeikis, H. Misawa, T. Tanimura, and K. Maeda, "Inverse silica opal photonic crystals for optical sensing applications," *Opt. Express* 15, 12979-12988 (2007).
- [7] I. M. White and X. Fan, "On the performance quantification of resonant refractive index sensors," *Opt. Express* 16, 1020-1028 (2008).
- [8] G. Z. Xiao, A. Adnet, Z. Y. Zhang, F. G. Sun, and C. P. Grover, "Monitoring changes in the refractive index of gases by means of a fiber optic Fabry-Perot interferometer sensor," *Sens. Actuators, A* 118, 177-182 (2005).
- [9] V. Bhatia, K. A. Murphy, R. O. Claus, M. E. Jones, J. L. Grace, T. A. Tran, and J. A. Greene, "Optical fiber based absolute extrinsic Fabry - Perot interferometric sensing system," *Meas. Sci. Technol.* 7, 58-61 (1996).
- [10] H. Xiao, J. Deng, G. Pickrell, R. G. May, and A. Wang, "Single-crystal sapphire fiber-based strain sensor for high-temperature applications," *J. Lightwave Technol.* 21, 2276-2283 (2003).
- [11] Y. Zhang, X. Chen, Y. Wang, K. L. Cooper, and A. Wang, "Microgap Multicavity Fabry-Pérot Biosensor," *J. Lightwave Technol.* 25, 1797-1804 (2007).
- [12] T. Wei, Y. Han, H-L. Tsai, and H. Xiao, "Miniaturized fiber inline Fabry-Perot interferometer fabricated with a femtosecond laser," *Opt. Lett.* 33, 536-538 (2008).
- [13] B. Qi, G. R. Pickrell, J. Xu, P. Zhang, Y. Duan, W. Peng, Z. Huang, W. Huo, H. Xiao, R. G. May, and A. Wang, "Novel data processing techniques for dispersive white light interferometer," *Opt. Eng.* 42, 3165-3171 (2003).
- [14] J. B. Hawkes, and R. W. Astherimer, "Temperature coefficient of the refractive index of water," *J. Opt. Soc. Am.* 38, 804-806 (1948).
- [15] Tao Wei, Yukun Han, Yanjun Li, Hai-Lung Tsai, and Hai Xiao, "Temperature-insensitive miniaturized fiber inline Fabry-Perot interferometer for highly sensitive refractive index measurement," *Opt. Express* 16, 5764-5769 (2008).